Impact of Assimilating Underwater Glider Data on Hurricane Gonzalo (2014) Forecasts

JILI DONG,[a,b] RICARDO DOMINGUES,[c,d] GUSTAVO GONI,[d] GEORGE HALLIWELL,[d]
HYUN-SOOK KIM,[a,b] SANG-KI LEE,[d] MICHAEL MEHARI,[c,d] FRANCIS BRINGAS,[d]
JULIO MORELL,[e] AND LUIS POMALES[e]

[a] I. M. System Group, Inc., Rockville, Maryland
[b] Marine Modeling and Analysis Branch, NOAA/Environmental Modeling Center, College Park, Maryland
[c] Cooperative Institute for Marine and Atmospheric Studies, University of Miami, Miami, Florida
[d] Physical Oceanography Division, NOAA/Atlantic Oceanographic and Meteorological Laboratory, Miami, Florida
[e] Department of Marine Sciences, University of Puerto Rico at Mayaguez, Mayaguez, Puerto Rico

ABSTRACT

The initialization of ocean conditions is essential to coupled tropical cyclone (TC) forecasts. This study investigates the impact of ocean observation assimilation, particularly underwater glider data, on high-resolution coupled TC forecasts. Using the coupled Hurricane Weather Research and Forecasting (HWRF) Model–Hybrid Coordinate Ocean Model (HYCOM) system, numerical experiments are performed by assimilating underwater glider observations alone and with other standard ocean observations for the forecast of Hurricane Gonzalo (2014). The glider observations are able to provide valuable information on subsurface ocean thermal and saline structure, even with their limited spatial coverage along the storm track and the relatively small amount of data assimilated. Through the assimilation of underwater glider observations, the prestorm thermal and saline structures of initial upper-ocean conditions are significantly improved near the location of glider observations, though the impact is localized because of the limited coverage of glider data. The ocean initial conditions are best represented when both the standard ocean observations and the underwater glider data are assimilated together. The barrier layer and the associated sharp density gradient in the upper ocean are successfully represented in the ocean initial conditions only with the use of underwater glider observations. The upper-ocean temperature and salinity forecasts in the first 48 h are improved by assimilating both underwater glider and standard ocean observations. The assimilation of glider observations alone does not make a large impact on the intensity forecast due to their limited coverage along the storm track. The 126-h intensity forecast of Hurricane Gonzalo is improved moderately through assimilating both underwater glider data and standard ocean observations.

1. Introduction

Interaction between the upper ocean and tropical cyclones (TCs) may partly drive further intensification or dissipation through several key feedback mechanisms such as the development of turbulent mixing, upwelling, and baroclinic adjustment processes (e.g., Price et al. 1994; Dickey et al. 1998; Prasad and Hogan 2007). While baroclinic adjustment processes (i.e., propagation of

inertial internal waves in the thermocline) provide one way of dispersing the energy introduced by hurricane winds in the ocean (Shay and Elsberry 1987; Brink 1989), turbulent mixing and upwelling may also lead to upper-ocean cooling, which is often linked to hurricane intensity changes and possibly dissipation (e.g., Glenn et al. 2016). The upper-ocean response and related air–sea interface variability are critical for TC development (Cione 2015).

Turbulent mixing is the main process leading to upper-ocean cooling, while hurricane-forced upwelling can also contribute to the cooling. The latter is manifested significantly for a slow-moving storm, in general less than ~4 m s^{-1} (Price 1981; Prasad and Hogan 2007; Yablonsky and Ginis 2009; Halliwell et al. 2015).

Nevertheless, there are occasions when specific characteristics of ocean conditions can suppress turbulent mixing and sea surface cooling. For example, the presence of barrier layers (Balaguru et al. 2012a; Grodsky et al. 2012; Domingues et al. 2015) and/or large upper-ocean heat content (Shay et al. 2000; Lin et al. 2008; Mainelli et al. 2008; Goni et al. 2016) can efficiently reduce storm-induced sea surface temperature (SST) cooling. Barrier layers are usually linked with low-salinity waters near the surface, associated with the heavy precipitation that accompanies a storm or freshwater discharge from the Amazon and Orinoco Rivers (e.g., Kelly et al. 2000; Corredor et al. 2003; Balaguru et al. 2012a; Johns et al. 2014). The low salinity values near the surface define strong stratification conditions that often exceed the effects of vertical shear (e.g., Domingues et al. 2015), and physically suppress turbulent mixing and SST cooling. When the effects of vertical shear exceed the influence of stratification, strong hurricane-forced SST cooling may sometimes be observed (Glenn et al. 2016).

Hurricane-forced upper-ocean cooling may subsequently lead to a reduction in the intensity of the storm by limiting air–sea fluxes of heat and moisture. This negative feedback mechanism is more effective for slower-moving storms (Halliwell et al. 2015), and for storms that travel over areas with low upper-ocean heat content, often referred to as tropical cyclone heat potential (TCHP) (Goni et al. 2009). TCHP is defined as the thermal energy required to increase the temperature above 26°C, integrated from the ocean surface to the depth of the 26°C isotherm. TCHP is considered a key factor affecting air–sea interaction in tropical cyclone forecasts (Mainelli et al. 2008; Goni et al. 2009; Lin et al. 2013). Areas with high TCHP and deep mixed layers require very strong turbulent shear to entrain sufficient thermocline waters to cool the mixed layer. In these areas, higher TCHP results favor hurricane intensification by suppressing SST cooling underneath the storm, and maintaining the surface sensible and latent heat fluxes from the ocean to the atmosphere (Lin et al. 2008; Mainelli et al. 2008). In fact, ocean observations and analyses showed that Hurricane Opal (1995) (Shay et al. 2000) and Hurricane Katrina (Mainelli et al. 2008) experienced rapid intensification [defined as a 30-kt increase (where $1 \, kt = 0.51 \, m \, s^{-1}$) in wind speed within 24 h] while traveling over anticyclonic features with high TCHP in the Gulf of Mexico.

Therefore, in order to improve hurricane intensity forecasts within a coupled atmosphere–ocean model, it is critical to provide ocean initial conditions that accurately represent the ocean thermal and saline structures (Chan et al. 2001; Emanuel et al. 2004; Wang and Wu 2004; Halliwell et al. 2015), particularly in the upper ocean. Underwater gliders (gliders hereafter) are an excellent observational platform for providing a large number of ocean profile observations with a rather flexible navigation and sampling strategy that can be adapted according to the projected storm track (Domingues et al. 2015). Gliders can be piloted along predetermined tracks and configured at any time to update the navigation and other relevant parameters, such as the spatial and temporal sampling strategy. Gliders can also effectively provide sustained and targeted ocean observations under hurricane force wind conditions, offering a cost-effective observational platform to complement other observations, such as Argo floats and airborne expendable bathythermographs (AXBTs). Many efforts have been made in recent years to assimilate glider data in regional or coastal ocean models to improve ocean initialization (Oke et al. 2009; Shulman et al. 2009; Dobricic et al. 2010; Zhang et al. 2010; Pan et al. 2011; Yaremchuk et al. 2011; Jones et al. 2012; Melet et al. 2012; Gangopadhyay et al. 2013; Mourre and Chiggiato 2014; Pan et al. 2014). Rudnick (2016) summarized some of the above data assimilation studies in a review paper. All of the studies demonstrated the positive impact of assimilating glider data on ocean forecasts.

This study focuses on the impact of assimilating glider observations on ocean initialization and hurricane prediction within the Hurricane Weather Research and Forecast (HWRF) Model–Hybrid Coordinate Ocean Model (HYCOM) coupled hurricane forecast system. This is the first study of its kind to investigate the impact of ocean observations on hurricane forecasting in this region using a convection-permitting atmosphere–ocean coupled hurricane model.

The case study presented in this manuscript focuses on Hurricane Gonzalo (2014), the strongest hurricane in the North Atlantic Ocean from 2011 to 2014. TC Gonzalo started to develop as a tropical storm in the tropical North Atlantic Ocean on 12 October 2014. The storm traveled to the west and developed into a category 1 hurricane on 13 October 2014. Gonzalo rapidly intensified into a category 3 hurricane on 14 October and continued to intensify into a category 4 hurricane on 15 October with maximum sustained winds of 115 kt (Brown 2015). Before Gonzalo started to recurve northeastward on 16 October, it experienced an eyewall replacement cycle and slightly weakened (Fig. 1) (Brown 2015). Gonzalo reached its peak intensity of 125 kt at 1200 UTC 16 October. After that stage, increasing wind shear and cooler SSTs weakened Gonzalo while it continued to accelerate north-northeastward (Brown 2015). The 126-h coupled model simulation
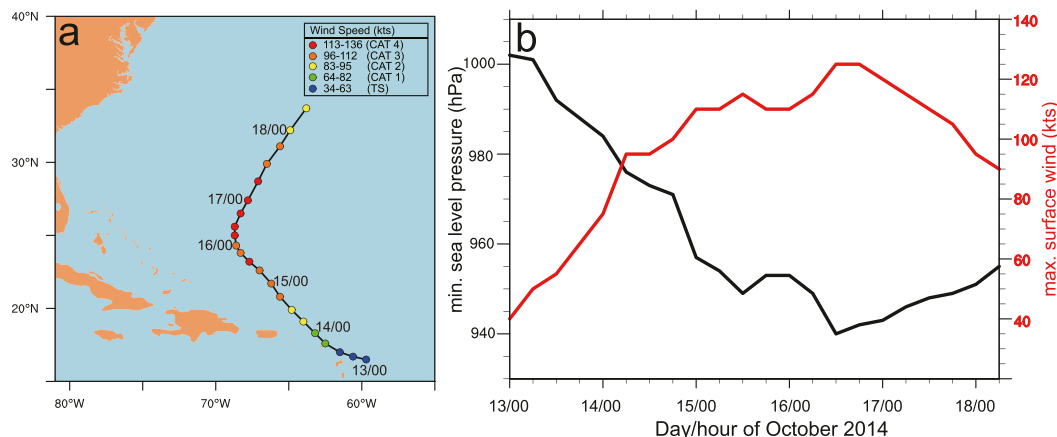
FIG. 1. (a) Track and (b) intensity [minimum sea level pressure (hPa) and surface maximum wind (kt)] of Hurricane Gonzalo (2014).

analyzed in this manuscript covers the rapid intensification of Gonzalo and its subsequent life cycle from 13 to 18 October.

This manuscript is organized as follows. The prestorm upper-ocean conditions before the passage of Gonzalo are discussed in section 2. Section 3 describes the coupled model, data assimilation system, experiment setup, and ocean observations. The impacts of glider observations on ocean initial conditions and subsequent ocean and hurricane forecasts are examined in sections 4 and 5, respectively. Section 6 provides a summary of this study.

2. Upper-ocean conditions during Hurricane Gonzalo (2014)

Two gliders were deployed in mid-July 2014 to sample the ocean conditions during the Atlantic hurricane season of 2014. One glider was deployed in the Caribbean Sea (not shown) and the other in the tropical North Atlantic (Fig. 2a). Both gliders were piloted along predetermined fixed tracks, obtaining approximately 12 temperature and salinity profiles per day between the surface and 1000-m depth. Temperature and salinity (T/S) profiles collected by the two gliders in October 2014 provided key profile observations of the upper-ocean structures before, during, and after the passage of Gonzalo. These data were assimilated into the HYCOM ocean model to assess the impact of glider data on HWRF–HYCOM forecasting skill.

During 8–13 October 2014, the glider traveled along section A–B, sampling prestorm temperature and salinity conditions between the surface and 1000-m depth. From 13 to 15 October, the glider was parked at location B to measure the ocean response during the passage of the storm. During its intensification to category 3, the

center of Hurricane Gonzalo was positioned at 20.8°N, 65.6°W, approximately 85 km northeast of glider location B, north of Puerto Rico (Fig. 2a). Prestorm temperature observations showed that there was an upper layer with a homogenous temperature of ~29°C above 50 m (Fig. 2b) and that the depth of the 26°C isotherm was located at about 90-m depth along the section A–B. It is estimated here that the TCHP in the region along section A–B was approximately $86 \, \mathrm{kJ \, cm^{-2}}$, well above the $50 \, \mathrm{kJ \, cm^{-2}}$ threshold for sustaining a hurricane in the tropical North Atlantic Ocean (Mainelli et al. 2008). Salinity observations (Fig. 2c) showed that, north of 20.6°N, a homogenous salinity layer with values of 36.7 psu was observed above 90 m. South of this latitude, a shallow low-salinity layer was observed above 20 m, with values as low as 35.8 psu at site B (Fig. 2e). The observed reduction in salinity leads to a strong density stratification above 50 m (Domingues et al. 2015; see Fig. 7 below).

Satellite-derived observations for 13 October 2014 indicate that warm surface waters with SSTs higher than 28.5°C (Fig. 8a) extended through a large area around the location of the glider and that Hurricane Gonzalo traveled most of the time over areas that had initial SSTs above 26°C (Fig. 8a). While most areas along the track of Gonzalo were initially associated with SSTs above 26°C, satellite-derived TCHP indicates that values above $60 \, \mathrm{kJ \, cm^{-2}}$ were mostly found south of 25°N (Fig. 8e), in agreement with the glider observations (section 4a). Larger hurricane-induced upper-ocean cooling is therefore expected north of this latitude (Lin et al. 2008).

Upper-ocean heat content observed along the track of Hurricane Gonzalo in October 2014 was anomalously high with respect to the historical record (Fig. 3). The
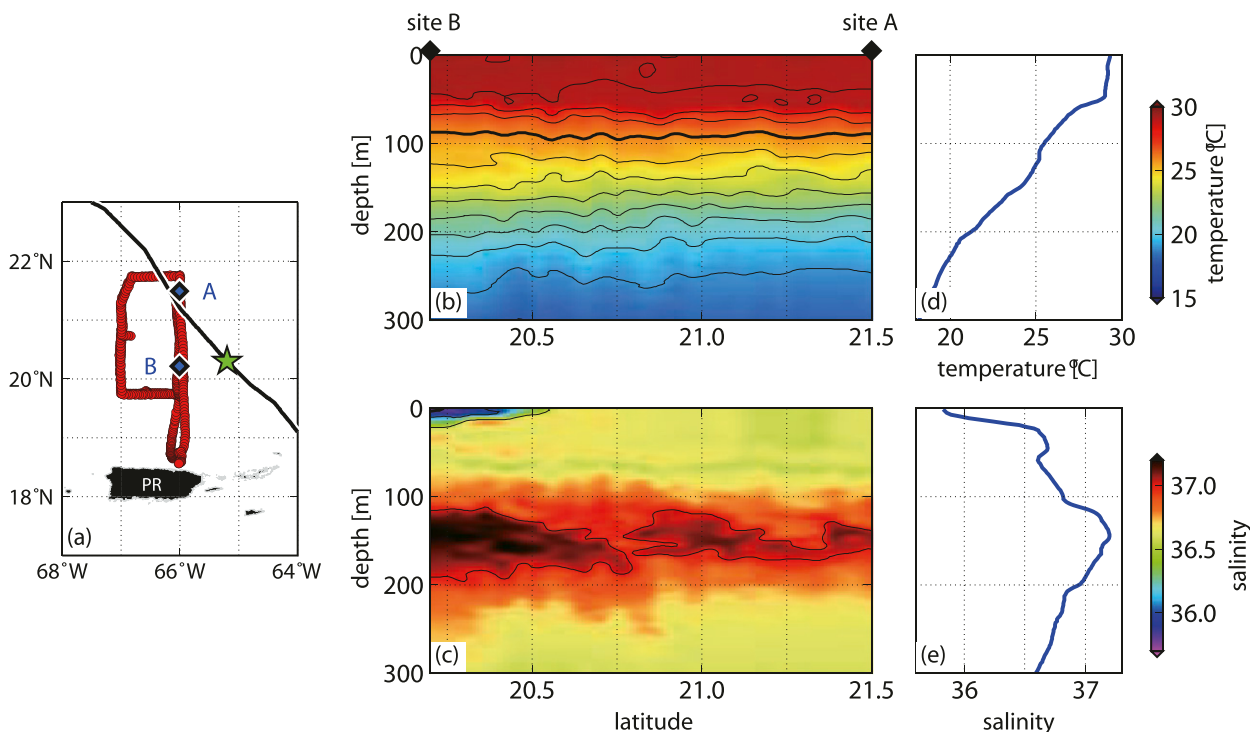
FIG. 2. (a) Location of underwater glider profile observations sampled north of PR during Jul–Nov 2014 (red dots). During 8–13 Oct 2014, the glider traveled along section A–B, sampling *T/S* conditions before the passage of Hurricane Gonzalo (black line). Prestorm (b) *T* and (c) *S* conditions between sites A and B. Initial (d) *T* and (e) *S* profiles at site B on 13 Oct 2014, before the passage of Hurricane Gonzalo.

space (latitude)–time diagram of sea height residuals (SHRs, annual cycle removed) along section A–B (Fig. 3a) shows that the signal is dominated by positive values of SHR starting in 2012. Positive SHRs are of special interest because they indicate warm monthly anomalies with respect to the upper-ocean heat content since 1993. In October 2014, SHRs reached values of 10 cm above the long-term average for October during the 1993–2015 period, suggesting that upper-ocean conditions were warmer than usual in this location. Analysis of TCHP residuals at site B during 1993–2015 (Fig. 3b) further indicates that the upper-ocean heat content in October 2014 was ~15 kJ cm^{-2} higher than the average conditions observed in this area.

The analysis above shows that ocean conditions during October 2014 were favorable overall for the development and potential intensification of Hurricane Gonzalo (2014). The presence of larger than average upper-ocean heat content and of a 20-m-thick barrier layer along the track of Gonzalo may have largely suppressed the hurricane-forced SST cooling. This cooling ranged between −0.4° and −1°C in the region sampled by the glider (Domingues et al. 2015) and peaked at −2°C when Hurricane Gonzalo reached its maximum intensity as a category 4 hurricane at 23.5°N, 68.0°W

(Goni et al. 2016). The small upper-ocean cooling caused by the hurricane may have favored further intensification.

3. Model and data assimilation experiment setup

a. The HWRF–HYCOM coupled model

The coupled model used in this study is the HWRF–HYCOM system, consisting of the atmospheric model HWRF and the ocean model HYCOM. The HWRF model is the operational numerical model for hurricane forecasting used by the Environmental Modeling Center (EMC) of the National Centers for Environmental Prediction (NCEP) and provides real-time tropical cyclone prediction during hurricane seasons. This model has three domains (27-, 9-, and 3-km horizontal resolutions) with the two nesting domains moving with a storm. HWRF solves the governing nonhydrostatic equations on the rotated latitude–longitude horizontal mesh and 63 hybrid pressure-sigma vertical layers extending up to 2 hPa. The physical parameterizations used in HWRF include cumulus convection in the intermediate and outer domains, Ferrier microphysics, a modified Global Forecast System (GFS) planetary
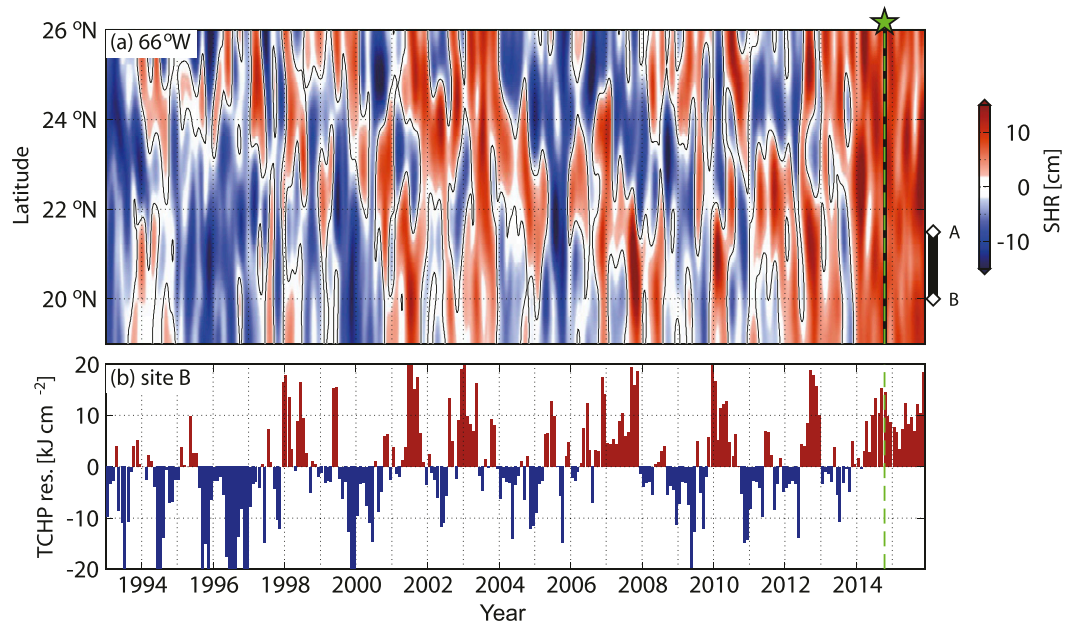
FIG. 3. (a) Latitude–time Hovmöller diagram for monthly SHRs (seasonal cycle removed) during 1993–2015 along section A–B. (b) Time series of TCHP residuals at site B during 1993–2015.

boundary layer (PBL), Rapid Radiative Transfer Model for general circulation models (RRTMG) long- and shortwave radiation, and HWRF surface flux (Soloviev et al. 2014). The details of the physical parameterizations can be found in the HWRF science document (Tallapragada et al. 2015).

The ocean model HYCOM has a single domain with a uniform horizontal resolution of $1/12°$ to cover the North Atlantic. This model has 32 hybrid vertical levels that include the terrain-following coordinate near the coast, the z coordinate in the mixed layers, and the isopycnal coordinate in deep water. The vertical mixing process is parameterized with the K-profile parameterization scheme (KPP). In the coupling system, HYCOM receives the wind stress, surface sensible and latent heat fluxes, net longwave and shortwave radiation, and precipitation from HWRF, while HYCOM feeds the SSTs to the HWRF model every 540 s of coupling time.

b. Experiment setup and observations

The atmospheric component model was initialized using the GFS analysis at 0000 UTC 13 October 2014. The initial storm was first relocated to the location of the National Hurricane Center best track. The vortex intensity and size are adjusted according to the storm message file or TC vitals, using the HWRF vortex initialization package. The initialization details can also be found in the HWRF scientific document (Tallapragada et al. 2015). The lateral boundary conditions of HWRF used in this work were derived from the GFS forecast.

No atmospheric data assimilation was performed in this study.

The ocean initial conditions were obtained from the ocean forecast–data assimilation cycle system maintained at the Physical Oceanography Division (PHOD) of the Atlantic Oceanographic and Meteorological Laboratory (AOML) of the National Oceanic and Atmospheric Administration (NOAA). The ocean data assimilation system used in this study employed a statistical interpolation method, where users can specify forecast/background error covariance flexibly (Halliwell et al. 2014). In this study, an ensemble of model states sampled at different times was used to represent the forecast error covariance (Halliwell et al. 2014).

Additional ocean observations assimilated, other than those obtained by the gliders, include along-track measurements of sea surface height anomaly (SSHA) from three satellite altimeters (*Jason-1*, *Jason-2*, and *Envisat*); SST from the satellite-derived multichannel SST (MCSST) product; in situ measurements collected by ships, surface buoys, and surface drifters; and temperature profile data from XBTs and Argo floats. An example of the distribution of these standard ocean observation distributions from different ocean observing platforms (from 29 September to 13 October 2014) is plotted in Fig. 4. The observation errors specified in the data assimilation system for each of the above types are the same as in Halliwell et al. (2014). All observations mentioned above are denoted as standard observations, as compared with glider observations. The localization or cutoff radii for each data type are also consistent with
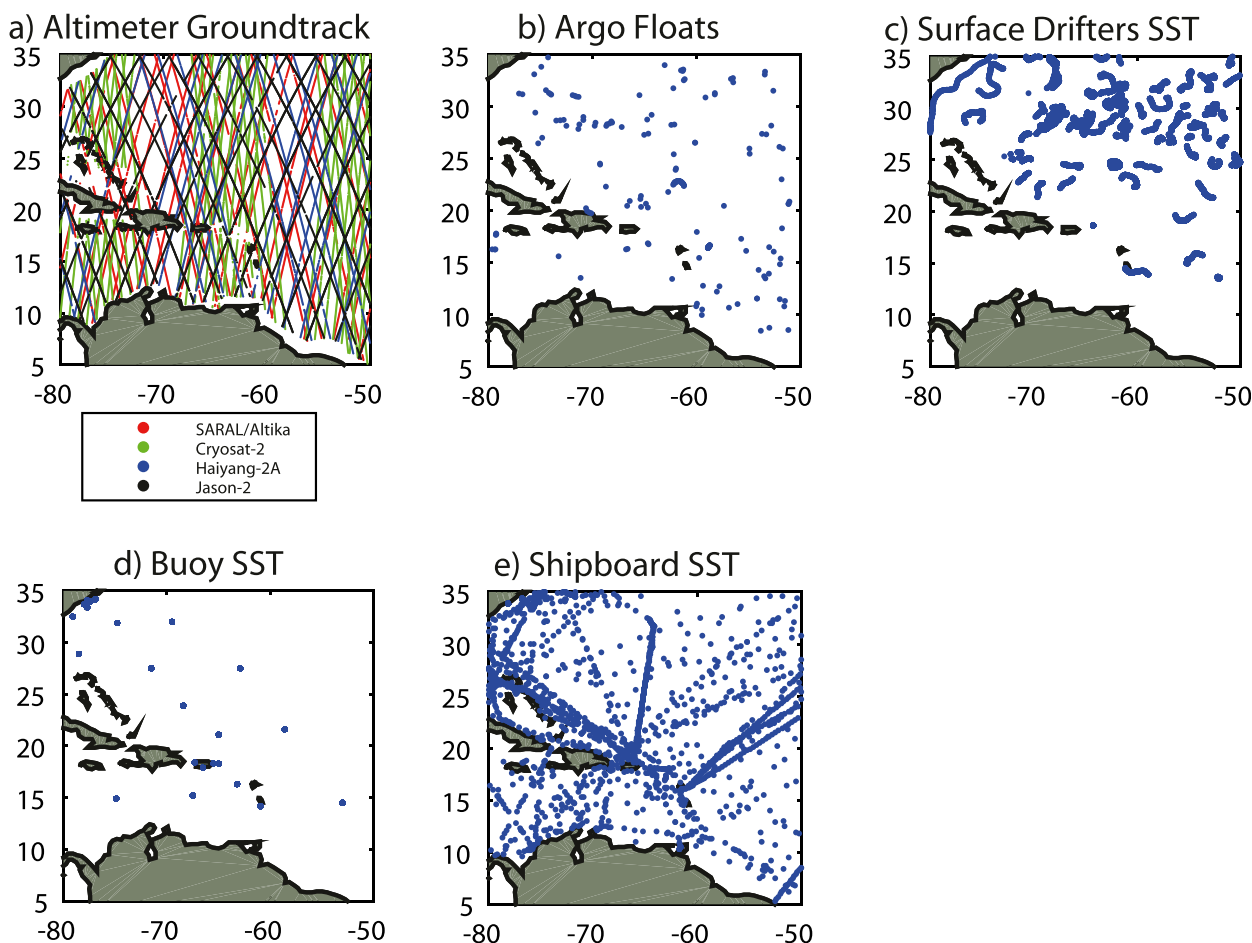
FIG. 4. Standard ocean observation distribution from 29 Sep to 13 Oct.

Table 3 of Halliwell et al. (2014). All standard observations were assimilated daily from 0000 UTC 1 March through 0000 UTC 13 October 2014. For the underwater glider T/S profiles, the observation error is 0.01°C for temperature and 0.02 psu for salinity. Among the T/S profile data from two gliders, only observations at 0000 UTC were assimilated from 0000 UTC 15 July to 0000 UTC 13 October 2014. The numbers of each observation type assimilated in this study are listed in Table 1.

In this study, an unconstrained ocean simulation from September 2008 through 2014, denoted as NODA, was used as the benchmark experiment. Three data assimilation experiments were designed to examine the impact of assimilating underwater glider T/S data and standard observations, and they are denoted as GLID (assimilation of glider data only), CTRL (assimilation of all ocean data except glider data), and ALL (assimilation of all ocean data) (Table 2). After the initialization of both atmospheric and ocean models, the 126-h coupled hurricane forecast is run from 0000 UTC 13 October until 0600 UTC 18 October, covering most of the life cycle of Gonzalo as a hurricane.

4. Impact of underwater gliders on initial ocean conditions

a. Impact of underwater glider observations on upper-ocean temperature and salinity structure

The prestorm upper-ocean thermal and saline structures directly affect the ocean response to hurricanes and the related SST cooling (Emanuel et al. 2004;

TABLE 1. Numbers of observations assimilated in this study. Observations ranged from 1 Mar to 13 Oct 2014 and were assimilated in the HYCOM model domain covering the North Atlantic.

Type of obs	No. of obs
Altimetry	1 283 123
Buoy SST	488 011
Shipboard SST	199 630
Drifter SST	1 360 046
Argo floats (profiles)	7562
AXBT (profiles)	1829
Glider (profiles)	180

TABLE 2. Data assimilation experiment setup. Details of observations can be found in section 3b.

Expt	Obs assimilated/remark
NODA	No obs
GLID	Two underwater gliders
CTRL	Standard ocean observations (Jason altimeter, MCSST, AXBT, AXCTD, Argo floats, surface drifters, etc.)
ALL	Gliders plus standard ocean observations

Yablonsky and Ginis 2009; Halliwell et al. 2015). The prestorm ocean conditions were sampled by the underwater glider while it was located at 20.2°N, 66°W, at 0000 UTC 13 October, about 781 km away from the eye of Gonzalo (16.5°N, 59.7°W). To examine the impact of assimilating underwater glider T/S data and other standard ocean observations on the prestorm upper-ocean conditions, the initial T/S conditions from four experiments at 0000 UTC 13 October were interpolated to the glider location and compared to the glider T/S profiles (Fig. 5), used here as the ground truth. The differences between model outputs and the glider observations (model − obs) were calculated (Fig. 6).

The prestorm ocean profile exhibited a mixed layer around 55 m deep and an SST of 29°C (black line in Fig. 5a). The temperature profile of NODA showed a much shallower mixed layer depth of 10 m and a negative bias across the upper 150 m of the ocean. The model SST was 0.2°C colder than the glider observations, with the surface-layer temperature showing a local maximum bias of −1.5°C at the observed mixed layer base of 55 m (Fig. 6a). The negative temperature bias continued to

increase from 65 m to the deeper ocean and reached values beyond −1.5°C below 100 m. The assimilation of glider T/S profiles in GLID improved the vertical thermal structure by reducing the bias throughout most of the upper 150 m (Fig. 6b). The SST of GLID was warmer than the observed by only 0.3°C, and the local maximum of the surface-layer temperature error was found at the mixed layer base, 0.9°C smaller than that of NODA. The bias was always below 0.4°C between 60 and 120 m and increased to 1°C down to 150 m. The temperature profile of CTRL is similar to GLID above the mixed layer base (55 m) and had a bias always higher than 0.5°C from 60 to 150 m (Fig. 6c), which suggests that the assimilation of other standard observations also improved the prestorm thermal structure, although not as much as assimilating the glider T/S profiles. The assimilation of glider data together with other standard observations further improved the initialization of the ocean thermal structure around the glider location, as the mixed layer depth of ALL was around 30 m, deeper than CTRL but still 25 m shallower than observed (Fig. 6d). The shallower mixed layer of the model simulations was partly due to the deficiency of the vertical mixing scheme and/or the data assimilation system, such as the static background covariance structure. The temperature bias in ALL was further reduced over most of the upper 150 m compared with CTRL. There was a 0.3°C degradation at 55 m of ALL over CTRL, which was probably caused by inaccurate background/forecast error covariance.

The TCHP estimated from glider observations at around 20.2°N, 66°W was approximately 86 kJ cm^{-2}. The TCHP values calculated from four experiments at
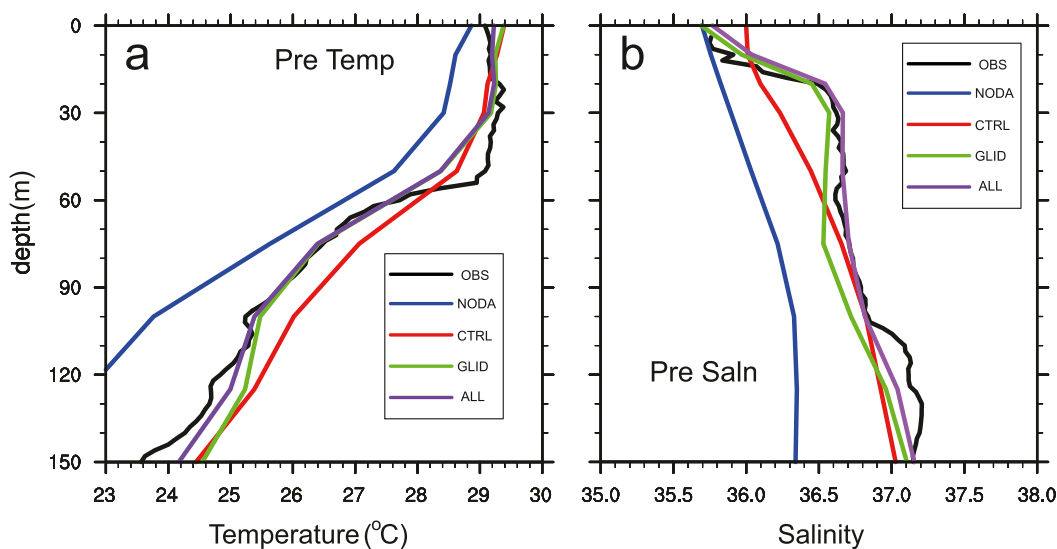

FIG. 5. (a) T and (b) S profiles at 0000 UTC 13 Oct 2014 from four experiments, compared with the glider observation.
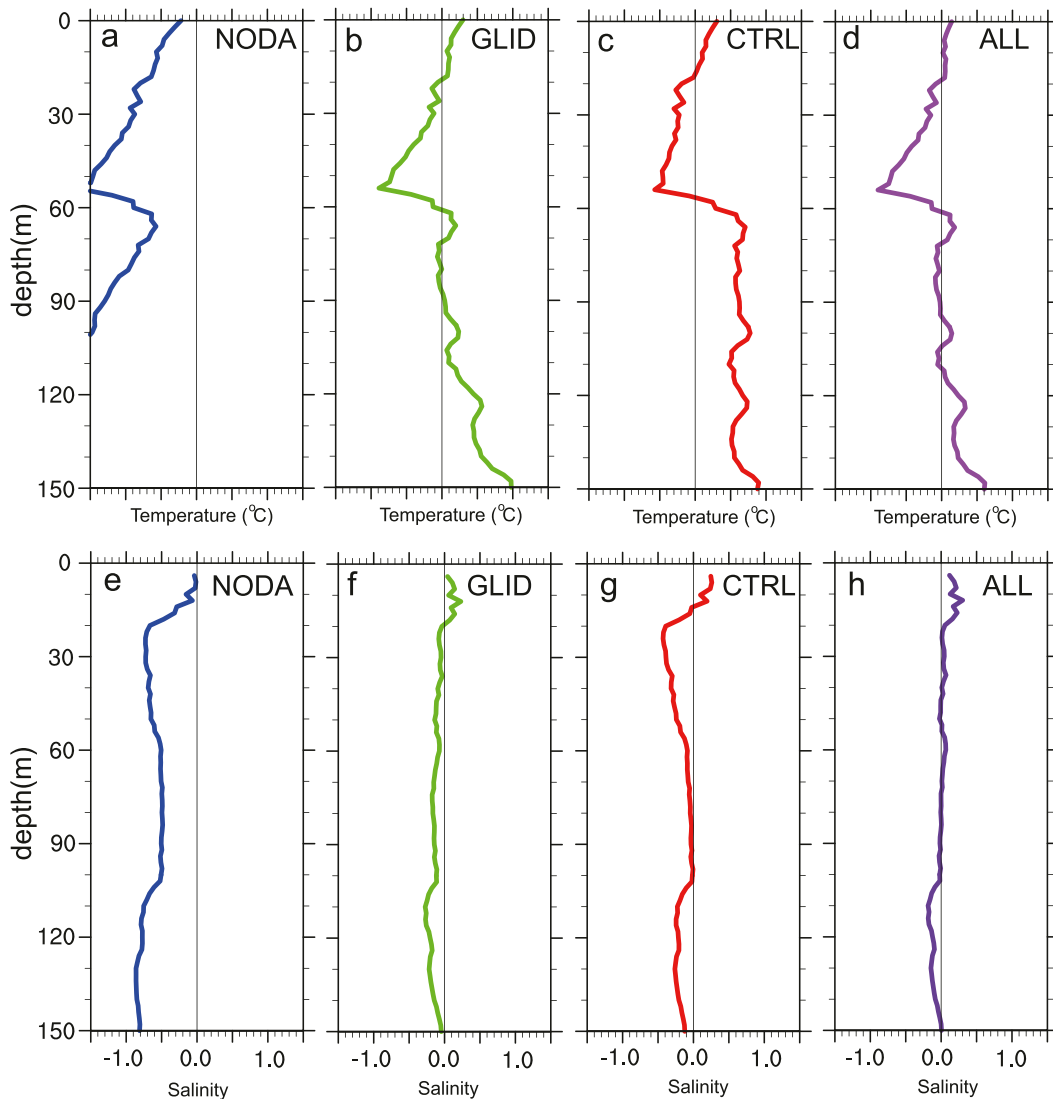
FIG. 6. (a)–(d) *T* (°C) and (e)–(h) *S* error profiles of four experiments (model − obs) at 0000 UTC 13 Oct 2014.

the glider location were 59, 81, 92, and 81 kJ cm^{-2} for NODA, GLID, CTRL, and ALL, respectively. The assimilation of glider observations greatly reduced the TCHP underestimate from 27 kJ cm^{-2} in NODA to 5 kJ cm^{-2} in GLID, reducing the percentage underestimate from 31% to 6%. Given that the threshold of TCHP for maintaining TC development is around 50 kJ cm^{-2} (Mainelli et al. 2008), an error reduction of 22 kJ cm^{-2} is notable and may translate into significant changes in the intensity forecast of Hurricane Gonzalo. While CTRL overestimated the TCHP by 6 kJ cm^{-2}, the additional assimilation of glider data led to a TCHP underestimation of 5 kJ cm^{-2} in ALL.

The saline structure is a key factor in determining the density field and, therefore, influences the vertical mixing that may affect TC intensification (Balaguru et al.

2012b; Domingues et al. 2015). The observed subsurface salinity quickly increased from the surface to 36.5 psu at 20 m (Fig. 5b). NODA underestimated the salinity with negative bias over 0.5 psu from 20 m down to 150-m depth (Fig. 6e). The assimilation of glider *T*/*S* data in either GLID or ALL greatly reduced the negative bias down to 0.2 psu (Figs. 6f,h). Assimilating the other standard observations also helped to reduce the error, although not as much as the assimilation of glider observations (Fig. 6g). The salinity of ALL was very close to the observations between 20 and 105 m with near-zero errors (Fig. 6h).

Accurate representation of upper-level density change, the barrier layer, and ocean stratification is essential to potentially improving the air–sea interaction and ocean feedback in the model and, in turn, the TC
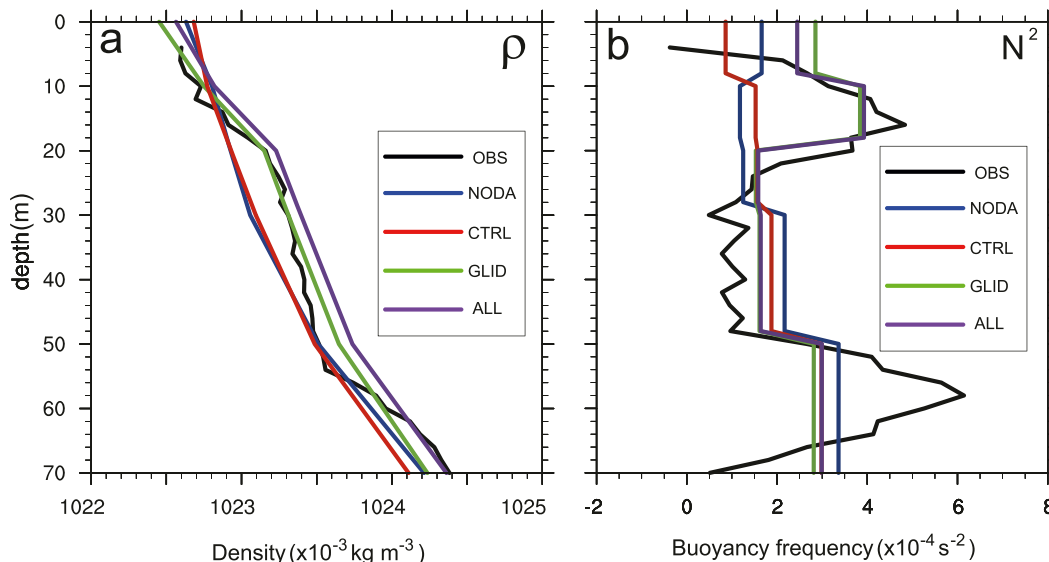
FIG. 7. As in Fig. 5, but for (a) density and (b) buoyancy frequency profiles.

forecast. The observed rapid salinity reduction from the surface to 20-m depth led to a sharp gradient of density over the shallow upper layers (Fig. 7a), forming a 20-m-thick barrier layer. The barrier layer, caused by the upper-layer salinity change, tends to resist vertical mixing and thus has the potential to reduce TC-forced SST cooling (Wang et al. 2011; Balaguru et al. 2012b). Balaguru et al. (2012b) showed that barrier layers can significantly influence TC intensification by modifying the SST cooling and air–sea heat flux exchange. This important feature of the density change and barrier layer was not well retrieved when ocean data were not assimilated (NODA). Assimilating other standard observations resulted in little improvement, with the density profile still smoothly increasing over the upper 50 m in both NODA and CTRL. On the other hand, with glider data assimilated in GLID and ALL (Figs. 7a,b), the sharp vertical density gradient was better retrieved in the upper 20 m, and the density profile of GLID over the upper 35 m was reasonably close to the observations (Fig. 7a). The improvement in the representation of the barrier layer and ocean stratification was also evident in assessing the buoyancy frequency N^2 (Fig. 7b). Large positive N^2, defined as the Brunt–Väisälä frequency, represents strong stability. The observations showed strong stability and stratification in the upper 20 m, which was better represented by the assimilation of glider data (GLID and ALL). The buoyancy frequencies of GLID and ALL were almost twice those of NODA and CTRL. The barrier layers in GLID and ALL were about 20 m thick and did not exist in NODA and CTRL.

In summary, the assimilation of underwater glider data improved ocean initialization by reducing the error of prestorm, upper-thermal and saline structures and producing a deeper isothermal layer and larger TCHP. The largest error reduction was mostly found below the mixed layer. One important result of the study, and applicable to this experiment only, is that the improvement from assimilating other standard observations is significant; however, it is not as large as that obtained from assimilating glider T/S data alone. Assimilating both standard and glider observations (ALL) appears to have the largest improvement on the upper-ocean initial conditions. Assimilation of glider data also improved the model representation of the upper-ocean density structure that included a barrier layer, which was accurately represented only when glider data were assimilated.

b. The impact of underwater glider observations on prestorm SST and TCHP

The impact of assimilating glider observations is not only limited to the exact location of the observations. The estimated forecast error covariance structure and localized radii combined determine how far the impact of observations will reach in a single cycle assimilation. Further forecast cycles will spread the impact of data assimilation even beyond the time and location of the assimilation. In this section, the initial large-scale ocean environment along the path of Gonzalo is briefly examined to assess how far and how large the impact of ocean data assimilation may reach. The values of SST and TCHP in the vicinity of the path of Gonzalo are of particular interest here.

Figure 8 shows the initial SST conditions for the three experiments at 0000 UTC 13 October 2014 overlapped with the 126-h predicted track of each storm. The best track is superimposed on the Remote Sensing Systems (RSS) SST fields retrieved from satellite microwave and IR products and optimally interpolated (OI) at 9-km resolution (Fig. 8a). The prestorm ocean conditions show a large body of warm water with SSTs over 28.5°C in the Caribbean Sea and southern region of the North Atlantic subtropical gyre, which is known as the Atlantic warm pool and is closely correlated with Atlantic hurricane activity (e.g., Wang and Lee 2007). Hurricane Gonzalo crossed over this warm pool region with SSTs above 29°C before and in the vicinity of the hurricane track recurvature, coinciding with the rapid intensification of the storm. When no observations were assimilated, the warm pool in NODA is weaker and smaller compared with the satellite-derived values. SSTs never exceeded 29°C around and along the storm track (Fig. 8b). The assimilation of glider data greatly helped to improve the warm pool around both glider locations and along the storm path (Fig. 8c). With standard observations assimilated in CTRL, the warm pool structure is much better retrieved in a larger area. The warm pool structure of the environment and along the storm path is close to those found among the observations in terms of both strength and coverage (Fig. 8d). The additional impact of the assimilation of glider data in ALL was relatively minor (not shown), as a result of the limited space covered by the glider observations.

The results presented above are also illustrated in Fig. 9. The initial SST along the projected 126-h path of each storm (0000 UTC 13 October–0600 UTC 18 October) is averaged within a radius of 84 km from the storm centers (about two radii of maximum wind R_{max}) (Fig. 9). From 6 to 90 h, the observed initial SST remained around 29°C, while NODA never reached 29°C along the storm path. When the glider data were assimilated, the averaged along-storm SST in GLID was largely corrected to the observed value in the region close to the glider location (dashed line). The largest reduction of SST error along the track forecast is around 0.7°C over NODA. The averaged initial SST value in CTRL follows the observations quite well from 18 to 96 h with a 0.4°C overestimation around 48 h on the projected storm path. This 0.4°C positive bias is corrected by assimilating the glider data in ALL.

The initial TCHPs from the model are also shown in Fig. 8 and compared with the TCHP field produced at AOML/PHOD. The latter product is calculated from the altimeter-derived vertical temperature profiles estimates in the upper ocean (Dong et al. 2015). The impact of assimilating glider observations data on the TCHP distribution is consistent with the conclusion on SST: GLID improves over NODA while the TCHP of CTRL is better initialized within a much larger area (Figs. 8e–h).

5. Impact of underwater glider data on the coupled forecast

a. Impact on ocean forecast

The ocean component of the coupled forecast system provides the necessary oceanic feedback to the hurricane. Correctly predicting the ocean processes under strong hurricane wind conditions is critical to improving the parameterization of air–sea interaction and hurricane forecasts. As shown in section 4a, the prestorm ocean T/S conditions were improved by the assimilation of underwater glider observations. We examine here whether the improvements will be maintained in the subsequent unconstrained ocean forecast by comparing the ocean forecasts with glider observations collected during the passage of Hurricane Gonzalo.

The observed ocean response to Hurricane Gonzalo obtained from the underwater glider data was discussed in Domingues et al. (2015). Between 0000 UTC 13 October and 0000 UTC 15 October, the underwater glider was parked at 20.2°N, 66°W (site B), providing a good opportunity to measure the in-storm ocean response. In this section, we mostly focus on the forecast error evolution of the four data (or no data) assimilation experiments during the 48-h period. The forecast error is defined here as the difference between the forecast and the glider data (model minus observation). The temperature and salinity error evolution of the upper 150-m depth is shown in Figs. 10 and 11, respectively.

Temperature errors in NODA are always negative with values above 0.6°C throughout the whole upper 150-m depth. The error changes little in the 2-day forecast (Fig. 10a). NODA also underestimates salinity (Fig. 11a) by at least 0.5 psu during most of the 48 forecast hours below 15-m depth. The assimilation of glider data significantly improves the initial T/S structure and also the subsequent ocean forecasts (Fig. 10b): forecast temperature error is clearly reduced above 30 m and the absolute error value is below 0.2°C during most of 2-day forecast in GLID. Below 60-m depth, the errors are also reduced. From 0800 UTC 13 October to 2000 UTC 14 October, the temperature error below 100 m in GLID is mostly under 0.4°C. The salinity forecast in GLID also generates a smaller error than NODA, mostly below 30-m depth (Fig. 11b). The magnitude of the salinity error largely remains below 0.3 psu. The
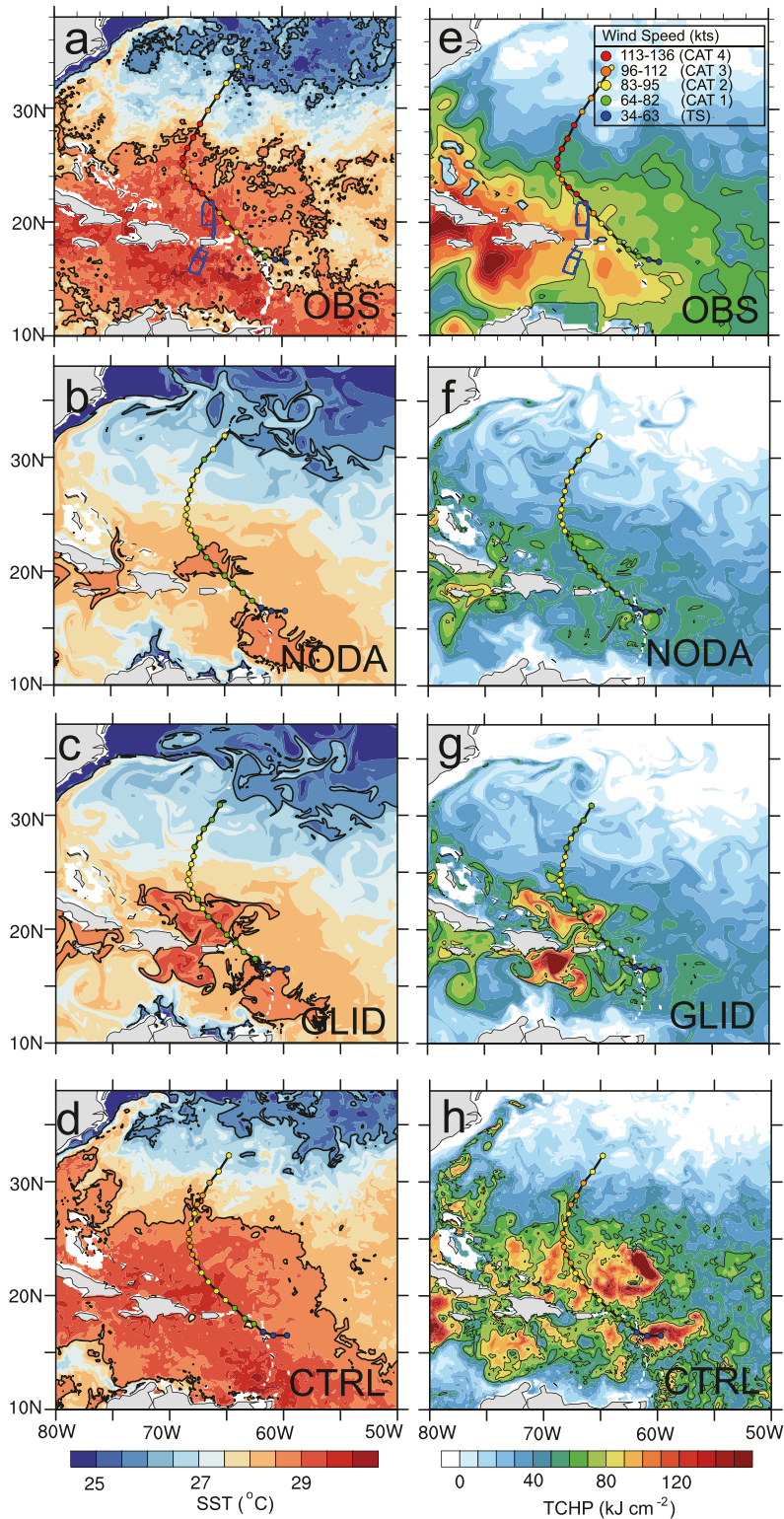
FIG. 8. (left) SST and (right) TCHP of (b),(f) NODA, (c),(g) GLID, and (d),(h) CTRL, along with (a),(e) the observations at 0000 UTC 13 Oct, overlapped with the best track in (a) and (e) or the predicted track of each individual experiment in (b)–(d) and (f)–(h). In (a)–(d) the 28.5° and 26°C isotherms are highlighted in SST plots. In (e)–(h) the 60 and 80 kJ cm^{-2} contours are highlighted in TCHP plots. The blue lines in (a) and (e) denote the locations of two underwater gliders deployed in 2014.
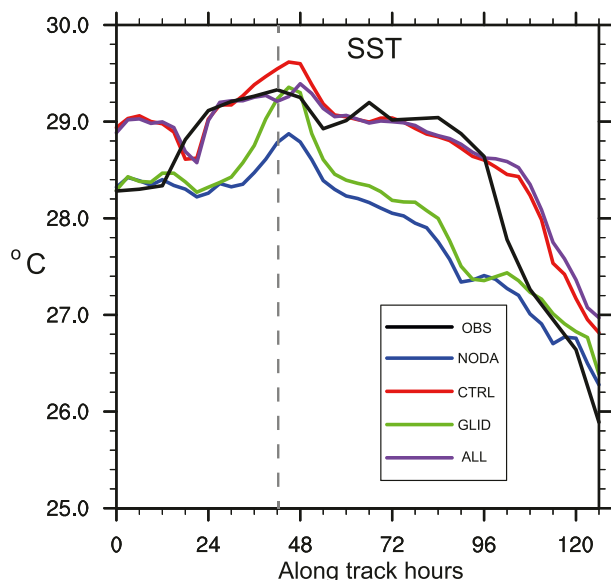
FIG. 9. SST of four experiments and remote sensing observations at 0000 UTC 13 Oct 2014, averaged along the best track (for observations) and the predicted future tracks (for four experiments) within a 84-km radius from the storm centers. The dashed line denotes the track location closest to the glider at 0000 UTC 13 Oct 2014.

assimilation of other standard ocean observations (CTRL) also helps to improve the ocean forecast (Figs. 10c and 11c). Temperature errors are greatly reduced above 40-m depth. Below the mixed layer, forecasts from CTRL have errors that are always positive in the 48-h forecasts in the upper thermocline (Fig. 11c). Similar to GLID, the salinity forecast in CTRL shows error reduction below 40-m depth, while the error between 40 and 100 m is generally smaller than in GLID (Fig. 11c). The additional assimilation of glider data in ALL further reduces both the temperature and salinity errors over CTRL (Figs. 10d and 11d). For temperature, the forecast error below 60 m is clearly reduced throughout the upper 150-m depth during most of the time for the 2-day forecast, and the error in the upper 30 m is slightly smaller than in CTRL (Fig. 10d). For salinity, the negative bias of CTRL in the upper 40 m is greatly reduced (Fig. 11d). The salinity error between 100- and 150-m depths also decreases, with the resulting error throughout the whole 150-m depth always below 0.3 psu during most of 48-h forecasts.

In general, the ocean forecast errors of temperature and salinity during the first 48 h are reduced by either the assimilation of glider data alone or by additional assimilation using other standard ocean observations when verified against the glider T/S observations. Among the four experiments examined in this study, the assimilation of both the standard ocean observations

and underwater glider data (e.g., all ocean observations available) produces the best ocean temperature and salinity forecasts in terms of error reduction.

b. Impact on Hurricane Gonzalo's forecast

We showed in section 4 that the assimilation of glider T/S data improves the upper-ocean thermal and saline conditions in areas that were directly under or in the proximity of the track of Hurricane Gonzalo. In this section, we will discuss the impact of initial ocean condition improvements on Hurricane Gonzalo forecasts in the coupled forecast system. To accomplish this, the track and intensity forecasts of Hurricane Gonzalo from different experiments will be examined.

The track forecasts of Gonzalo from the four experiments are shown in Fig. 12a, along with the observed best track. Gonzalo first moved to the northwest and along the southwest edge of the North Atlantic subtropical gyre. After staying over the warm waters of the Antilles current, Gonzalo started to recurve slowly toward the northeast at 1200 UTC 16 October. It continued to move northeast and weakened along the path until 0600 UTC 18 October. The predicted tracks follow the best track closely except for the last 36 h of the period when all the predicted storms move slower than the best track. Most of the predicted tracks exhibit a southward displacement during the first 54 h and an eastward bias by forecast hour 90. Tropical storm translation speed is crucial for controlling the underlying ocean response and the subsequent SST cooling feedback to the storm (Lin et al. 2009; Mei et al. 2012; Halliwell et al. 2015). The average 126-h translation speeds of the four experiments are 5.0, 5.1, 4.7, and 4.9 m s^{-1}, respectively, slightly slower than the 5.4 m s^{-1} of the best track and statistically equivalent, all indicating intermediate translation speeds [between 4 and 6 m s^{-1}; Mei et al. (2012)]. The difference among the track forecasts from the four experiments is relatively small, suggesting the ocean data assimilation has little impact on the track forecast and/or a relatively high predictability of track forecasts in this particular case. Since TC track forecasting is largely dependent on steering flow (Chan 2005, 2009), the small track spread among the experiments suggests that the large-scale atmospheric circulation is not significantly altered by the underlying ocean in the relatively short forecast period (126 h) for this particular case. The initial atmospheric conditions are identical in all four experiments, and they all use the same GFS boundary conditions.

To assess the intensity forecasts, the 126-h minimum sea level pressure and maximum surface wind forecasts of Gonzalo are evaluated (Figs. 12b,c). The actual storm intensified quickly in the first 60 h from a tropical storm
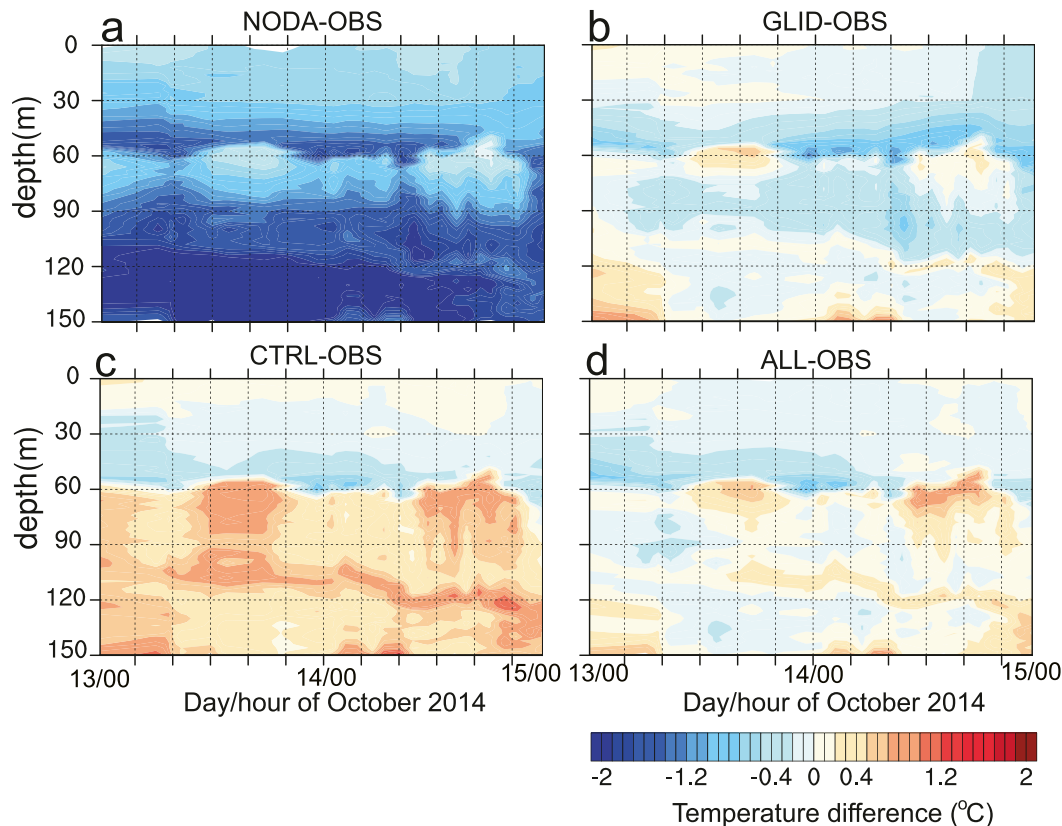
FIG. 10. Ocean temperature errors of (a) NODA, (b) GLID, (c) CTRL, and (d) ALL with depth during 0000 UTC 13 Oct–0000 UTC 15 Oct at 20.2°N, 66°W.

with a center pressure of 1002 hPa and maximum surface wind of 40 kt at 0000 UTC 13 October (16.5°N, 59.7°W) to a category 3 major hurricane with 949-hPa center pressure and 115-kt wind at 1200 UTC 15 October (23.2°N, 67.7°W). Gonzalo continued to intensify over the next 24 h into a category 4 hurricane with a 940-hPa center pressure and 125-kt wind at 1200 UTC 16 October (25.6°N, 68.7°W), which was also the strongest stage of the life cycle of this storm.

When there are no ocean observations assimilated (NODA), the forecast model fails to predict the rapid intensification of Gonzalo (Figs. 12b,c). The predicted storm slowly intensified and the forecasted center pressure and surface maximum wind are always weaker than the best track after 30 h. The strongest storm peak predicted in NODA has a center pressure of 957 hPa and maximum surface wind of 90 kt, which is only a category 2 hurricane. The assimilation of the data from the underwater gliders in GLID has little impact on the intensity forecast with small differences in both the center pressure and maximum wind between NODA and GLID. The intensity forecast is considerably improved by the assimilation of other standard ocean observations

in CTRL. CTRL predicts a rapid intensification of Gonzalo with the predicted center pressure of Gonzalo up to 13 hPa deeper than the best track during 12–48 h. The center pressure of CTRL after 0000 UTC 15 October is much closer to that from the best track, and the largest difference is more than 15 hPa stronger than for NODA. The peak intensity of CTRL reaches 943 hPa and 103 kt, making it a category 3 hurricane. The additional assimilation of underwater glider data in ALL shows a slight improvement over CTRL. The intensity of ALL further deepens to 939 hPa and 107 kt, with larger improvement over CTRL for the maximum wind during 78–108-h forecasts than during other forecast hours. This result suggests that assimilating glider data, if added to the existing observations, makes a larger impact on the intensity forecast of Hurricane Gonzalo than assimilating glider data alone. The limited coverage of glider observations, and the relatively small number of glider observations assimilated along the storm track, make the impact of assimilating glider observations much less significant than the impact of assimilating standard ocean observations.
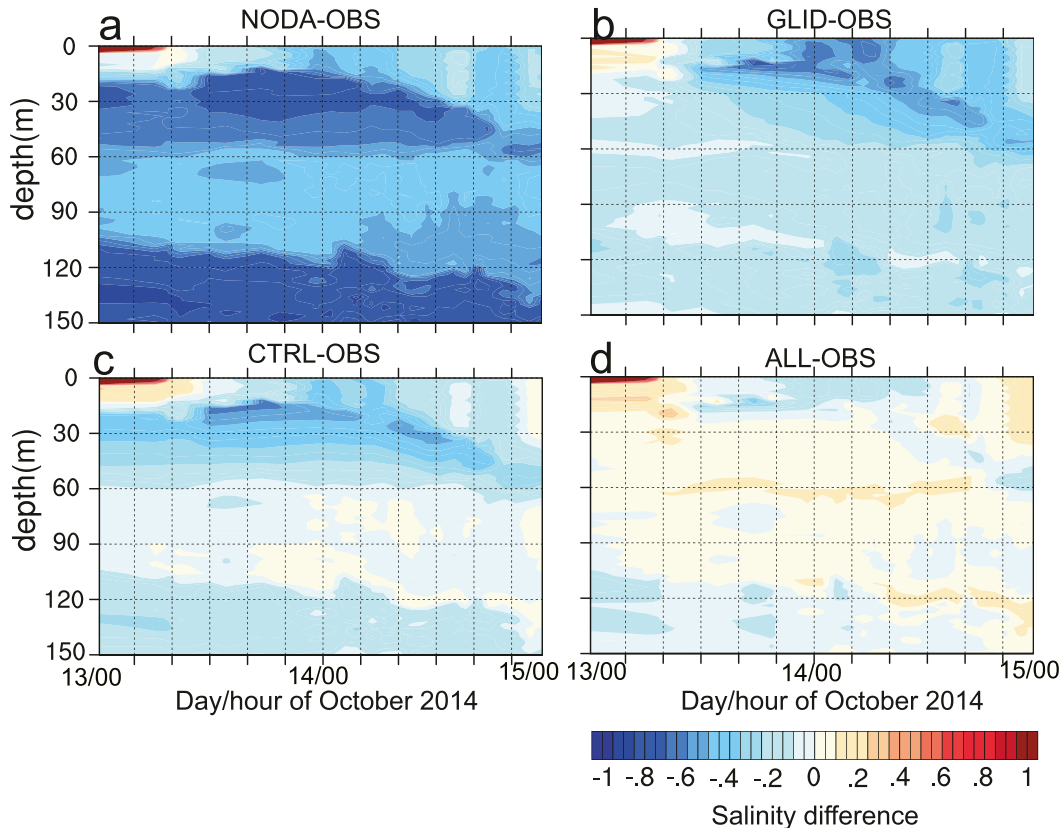
FIG. 11. As in Fig. 10, but for salinity errors.

It is also noticed that the predicted maximum surface wind from the coupled model forecasts always falls below the observations with a negative bias, although the central pressure is more or less comparable to the best track. This inconsistency is observed when the model overestimates the storm size so that a storm with the same center pressure but a larger size will produce smaller pressure gradients and weaker winds. Studies on how to improve TC size predictions are still ongoing and a better understanding of the physical processes related to TC intensification will help to improve these forecasts.

6. Conclusions

This study aims to investigate the impact of underwater glider observation assimilation on hurricane forecasts using a high-resolution coupled atmospheric–ocean numerical model system. Within this context, the ocean initialization and data assimilation are critical to providing an accurate picture of the ocean status for the coupled forecast. The hypothesis of this work is that underwater gliders provide a flexible sampling strategy and have the potential to improve hurricane forecasts by

representing a more accurate ocean structure for the coupled system. Hurricane Gonzalo (2014) was selected as the study case, because the ocean conditions were favorable for hurricane intensification.

The prestorm ocean thermal conditions in October 2014 are first compared with those of previous years. This comparison shows that the prestorm upper-ocean temperatures during October 2014 were higher than average and, thus, had the potential for TC development and intensification.

Results obtained here for this particular case study show that when the T/S data extracted from underwater gliders are assimilated, either alone or together with standard ocean observations, the prestorm ocean thermal and saline structures are significantly improved. The improvement in prestorm ocean SST is not limited to the exact location of the glider but also extends to areas surrounding the observations. It is also observed that the mixed layer depth, although improved by the assimilation of glider data, is still shallower than the observations. This is probably caused by simplified assumptions and inaccurate horizontal and vertical covariance of the statistical interpolation approach. More advanced data assimilation methods (e.g., variational or
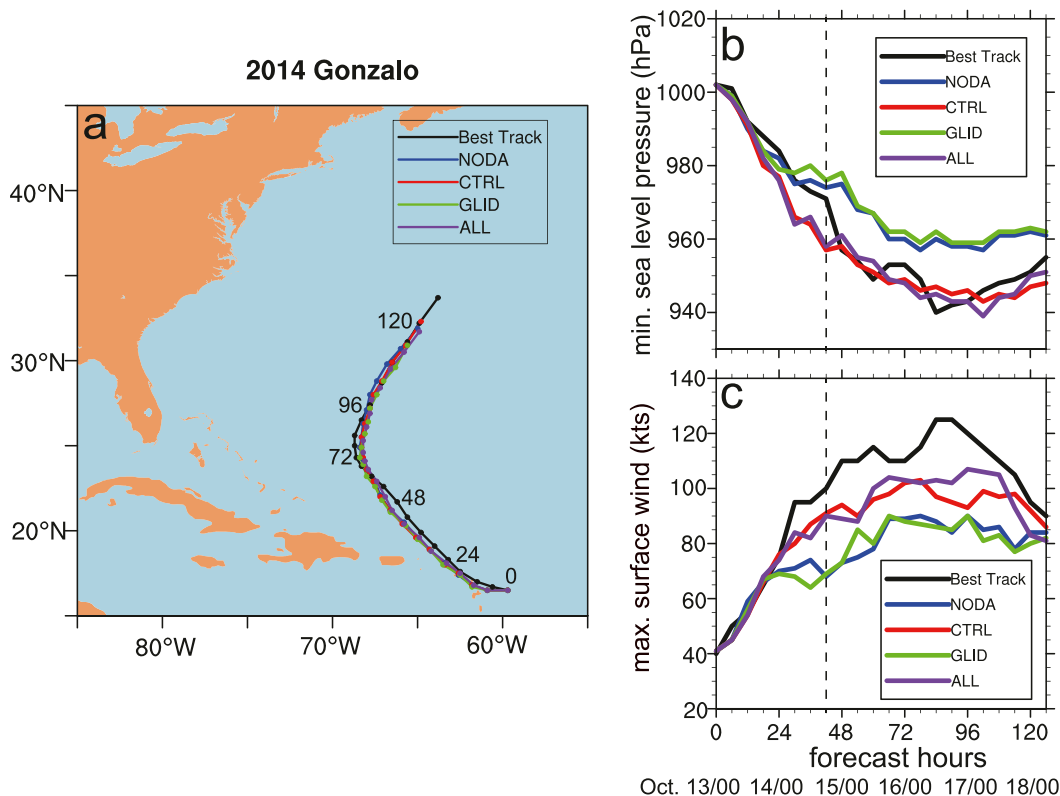
FIG. 12. (a) Hurricane Gonzalo track forecast, (b) minimum sea level pressure (center pressure), and (c) maximum wind forecasts, along with the best track. The dashed lines in (b) and (c) are the same as in Fig. 9.

ensemble-based data assimilation) may help to alleviate the problem.

The improvement in the initial saline structure from the assimilation of underwater glider data leads to better initialization of ocean density structures. The sharp density gradient and the related barrier layer are well represented only when underwater glider observations are assimilated. This improvement on the barrier layer and density structure proves the importance of glider data assimilation in initializing ocean conditions.

Our analysis shows that the assimilation of the standard ocean observations improves the intensity forecast of Gonzalo, having smaller errors in minimum center pressure and maximum surface wind. However, the assimilation of underwater glider observations alone does not have a significant impact on the intensity forecast. As Halliwell et al. (2015) demonstrated with very idealized one-dimensional ocean coupling forecast experiments, storms with intermediate translation speeds are less sensitive to the changes in TCHP than slow-moving storms (their Fig. 4). Furthermore, their study has shown the TC response to changes in the ocean thermal structure is gradual: for small storms moving at an intermediate speed, it may take 12 h for the adjustment to

become completely substantial after the storm eye passes the cool–hot ocean boundary. The above study suggests that changes in storm intensity are highly dependent on the horizontal scale of ocean features along the storm track: the storm has to stay over a particular ocean feature long enough (e.g., more than 12 h) to be effectively influenced. In our case study with Gonzalo, which is a relatively small storm with intermediate translation speed, the impact of assimilating glider observations may still be too localized along the storm track to affect the storm intensity significantly (Fig. 9). On the other hand, the other standard ocean observations, especially satellite altimeter observations, cover a large area over the full storm track (Fig. 4) and produce a significant improvement of the intensity forecast. Additional glider observations, if deployed along the storm tracks, may help to improve the ocean conditions covering a larger area and thus affect the intensity more efficiently.

The ocean forecasts produced by the coupled system are improved by assimilating glider observations by largely reducing both the temperature and salinity forecast errors near the glider location. The assimilation of both standard and glider observations produces the

best ocean forecast and characterization, when compared with the glider *T/S* observations. Results presented here indicate that for this case study the combination of glider data and standard ocean observations leads to the best hurricane intensity and ocean forecast, highlighting the impact of assimilating surface and profile ocean observations to improve the coupled hurricane intensity forecast.

Our investigation of ocean data assimilation on hurricane forecasts has shown promising results as the key step in addressing this challenging topic. More TC cases will be examined to obtain a rigorous conclusion on the role of ocean observations with different sampling strategies for the coupled TC forecast.

Compared with other standard ocean observations, the innovative glider observations still have a limited amount of spatial coverage and the number of observations available is relatively small so far, as shown in Table 1. A larger impact from glider assimilation was observed when combined with the standard ocean observations in this particular case. Notwithstanding the limited spatial coverage of glider observations, assimilation of glider data is still able to provide valuable information on subsurface thermal and saline structures of the ocean for coupled TC forecasts that is vital for model evaluation and improvement efforts. A similar procedure in the project supporting this study will be performed to extend the glider network: once the areas where hurricanes have historically intensified are identified, a well-designed glider network will be deployed. The collected data will then be assimilated to drive the coupled forecast for selected TC cases, and their impact will be evaluated. This approach will be first tested within an observing system simulation experiment (OSSE) framework. A network of 12–18 gliders will be simulated and assimilated for multiple TC cases within the OSSE framework, and their impact will be assessed. Future studies will also examine the individual impacts of temperature and salinity profile data from gliders on ocean initialization and TC forecasting. A more advanced data assimilation system (e.g., utilizing variational or ensemble-based data assimilation techniques) is also expected to help further maximize the ocean observations' impact.

REFERENCES

Balaguru, K., P. Chang, R. Saravanan, and C. J. Jang, 2012a: The barrier layer of the Atlantic warm pool: Formation mechanism and influence on the mean climate. *Tellus*, **64A**, 18162, doi:10.3402/tellusa.v64i0.18162.

——, ——, ——, L. R. Leung, Z. Xu, M. Li, and J.-S. Hsieh, 2012b: Ocean barrier layers' effect on tropical cyclone intensification. *Proc. Natl. Acad. Sci. USA*, **109**, 14 343–14 347, doi:10.1073/pnas.1201364109.

Brink, K. H., 1989: Observations of the response of thermocline currents to a hurricane. *J. Phys. Oceanogr.*, **19**, 1017–1022, doi:10.1175/1520-0485(1989)019<1017:OOTROT>2.0.CO;2.

Brown, D. P., 2015: Tropical cyclone report: Hurricane Gonzalo (AL082014). National Hurricane Center, 30 pp. [Available online at http://www.nhc.noaa.gov/data/tcr/AL082014_Gonzalo.pdf.]

Chan, J. C. L., 2005: The physics of tropical cyclone motion. *Annu. Rev. Fluid Mech.*, **37**, 99–128, doi:10.1146/annurev.fluid.37.061903.175702.

——, 2009: Movement of tropical cyclones. *Global Perspectives on Tropical Cyclones—From Science to Mitigation*, J. C. L. Chan and J. Kepert, Eds., World Scientific, 133–148.

——, Y. Duan, and L. K. Shay, 2001: Tropical cyclone intensity change from a simple ocean–atmosphere coupled model. *J. Atmos. Sci.*, **58**, 154–172, doi:10.1175/1520-0469(2001)058<0154:TCICFA>2.0.CO;2.

Cione, J., 2015: The relative roles of the ocean and atmosphere as revealed by buoy air–sea observations in hurricanes. *Mon. Wea. Rev.*, **143**, 904–913, doi:10.1175/MWR-D-13-00380.1.

Corredor, J., J. Morell, J. López, R. Armstrong, A. Dieppa, C. Cabanillas, A. Cabrera, and V. Hensley, 2003: Remote continental forcing of phytoplankton biogeochemistry: Observations across the "Caribbean-Atlantic front." *Geophys. Res. Lett.*, **30**, 2057, doi:10.1029/2003GL018193.

Dickey, T., and Coauthors, 1998: Upper-ocean temperature response to Hurricane Felix as measured by the Bermuda Testbed Mooring. *Mon. Wea. Rev.*, **126**, 1195–1201, doi:10.1175/1520-0493(1998)126<1195:UOTRTH>2.0.CO;2.

Dobricic, S., N. Pinardi, P. Testor, and U. Send, 2010: Impact of data assimilation of glider observations in the Ionian Sea (Eastern Mediterranean). *Dyn. Atmos. Oceans*, **50**, 78–92, doi:10.1016/j.dynatmoce.2010.01.001.

Domingues, R., and Coauthors, 2015: Upper ocean response to Hurricane Gonzalo (2014): Salinity effects revealed by targeted and sustained underwater glider observations. *Geophys. Res. Lett.*, **42**, 7131–7138, doi:10.1002/2015GL065378.

Dong, S., G. Goni, and F. Bringas, 2015: Temporal variability of the Meridional Overturning Circulation in the South Atlantic between 20°S and 35°S. *Geophys. Res. Lett.*, **42**, 7655–7662, doi:10.1002/2015GL065603.

Emanuel, K., C. DesAutels, C. Holloway, and R. Korty, 2004: Environmental control of tropical cyclone intensity. *J. Atmos. Sci.*, **61**, 843–858, doi:10.1175/1520-0469(2004)061<0843:ECOTCI>2.0.CO;2.

Gangopadhyay, A., A. Schmidt, L. Agel, O. Schofield, and J. Clark, 2013: Multiscale forecasting in the western North Atlantic: Sensitivity of model forecast skill to glider data assimilation. *Cont. Shelf Res.*, **63** (Suppl.), S159–S176, doi:10.1016/j.csr.2012.09.013.

Glenn, S. M., and Coauthors, 2016: Stratified coastal ocean interactions with tropical cyclones. *Nat. Commun.*, **7**, 10887, doi:10.1038/ncomms10887.

Goni, G., and Coauthors, 2009: Applications of satellite-derived ocean measurements to tropical cyclone intensity forecasting. *Oceanography*, **22**, 190–197, doi:10.5670/oceanog.2009.78.

——, J. A. Knaff, and I.-I. Lin, 2016: Tropical cyclone heat potential [in "State of the Climate in 2015"]. *Bull. Amer. Meteor. Soc.*, **96** (8), S120–S122, doi:10.1175/2016BAMSStateoftheClimate.1.

Grodsky, S. A., and Coauthors, 2012: Haline hurricane wake in the Amazon/Orinoco plume: AQUARIUS/SACD and SMOS observations. *Geophys. Res. Lett.*, **39**, L20603, doi:10.1029/2012GL053335.

Halliwell, G. R., Jr., A. Srinivasan, V. Kourafalou, H. Yang, D. Willey, M. L. Hénaff, and R. Atlas, 2014: Rigorous evaluation of a fraternal twin ocean OSSE system for the open Gulf of Mexico. *J. Atmos. Oceanic Technol.*, **31**, 105–130, doi:10.1175/JTECH-D-13-00011.1.

——, S. Gopalakrishnan, F. Marks, and D. Willey, 2015: Idealized study of ocean impacts on tropical cyclone intensity forecasts. *Mon. Wea. Rev.*, **143**, 1142–1165, doi:10.1175/MWR-D-14-00022.1.

Johns, E. M., and Coauthors, 2014: Amazon River water in the northeastern Caribbean Sea and its effect on larval reef fish assemblages during April 2009. *Fish. Oceanogr.*, **23**, 472–494, doi:10.1111/fog.12082.

Jones, E. M., P. R. Oke, F. Rizwi, and L. M. Murray, 2012: Assimilation of glider and mooring data into a coastal ocean model. *Ocean Modell.*, **47**, 1–13, doi:10.1016/j.ocemod.2011.12.009.

Kelly, P. S., K. M. M. Lwiza, R. K. Cowen, and G. J. Goni, 2000: Low-salinity pools at Barbados, West Indies: Their origin, frequency, and variability. *J. Geophys. Res.*, **105**, 19 699–19 708, doi:10.1029/1999JC900328.

Lin, I.-I., C.-C. Wu, I.-F. Pun, and D.-S. Ko, 2008: Upper-ocean thermal structure and the western North Pacific category 5 typhoons. Part I: Ocean features and the category 5 typhoons' intensification. *Mon. Wea. Rev.*, **136**, 3288–3306, doi:10.1175/2008MWR2277.1.

——, I.-F. Pun, and C.-C. Wu, 2009: Upper-ocean thermal structure and the western North Pacific category 5 typhoons. Part II: Dependence on translation speed. *Mon. Wea. Rev.*, **137**, 3744–3757, doi:10.1175/2009MWR2713.1.

——, G. J. Goni, J. A. Knaff, C. Forbes, and M. M. Ali, 2013: Ocean heat content for tropical cyclone intensity forecasting and its impact on storm surge. *Nat. Hazards*, **66**, 1481–1500, doi:10.1007/s11069-012-0214-5.

Mainelli, M., M. DeMaria, L. K. Shay, and G. Goni, 2008: Application of oceanic heat content estimation to operational forecasting of recent Atlantic category 5 hurricanes. *Wea. Forecasting*, **23**, 3–16, doi:10.1175/2007WAF2006111.1.

Mei, W., C. Pasquero, and F. Primeau, 2012: The effect of translation speed upon the intensity of tropical cyclones over the tropical ocean. *Geophys. Res. Lett.*, **39**, L07801, doi:10.1029/2011GL050765.

Melet, A., J. Verron, and J. M. Brankart, 2012: Potential outcomes of glider data assimilation in the Solomon Sea: Control of the water mass properties and parameter estimation. *J. Mar. Syst.*, **94**, 232–246, doi:10.1016/j.jmarsys.2011.12.003.

Mourre, B., and J. Chiggiato, 2014: A comparison of the performance of the 3-D super-ensemble and an ensemble Kalman filter for short-range regional ocean prediction. *Tellus*, **66A**, 21640, doi:10.3402/tellusa.v66.21640.

Oke, P. R., P. Sakov, and E. Schulz, 2009: A comparison of shelf observation platforms for assimilation in an eddy-resolving ocean model. *Dyn. Atmos. Oceans*, **48**, 121–142, doi:10.1016/j.dynatmoce.2009.04.002.

Pan, C., M. Yaremchuk, and D. Nechaev, 2011: Variational assimilation of glider data in the Monterey Bay. *J. Mar. Res.*, **69**, 331–346, doi:10.1357/002224011798765259.

——, L. Zheng, R. H. Weisberg, Y. Liu, and C. E. Lembke, 2014: Comparisons of different ensemble schemes for glider data assimilation on West Florida Shelf. *Ocean Modell.*, **81**, 13–24, doi:10.1016/j.ocemod.2014.06.005.

Prasad, T. G., and P. J. Hogan, 2007: Upper-ocean response to Hurricane Ivan in a 1/25° nested Gulf of Mexico HYCOM. *J. Geophys. Res.*, **112**, C04013, doi:10.1029/2006JC003695.

Price, J. F., 1981: Upper ocean response to a hurricane. *J. Phys. Oceanogr.*, **11**, 153–175, doi:10.1175/1520-0485(1981)011<0153:UORTAH>2.0.CO;2.

——, T. B. Sanford, and G. Z. Forristall, 1994: Forced stage response to a moving hurricane. *J. Phys. Oceanogr.*, **24**, 233–260, doi:10.1175/1520-0485(1994)024<0233:FSRTAM>2.0.CO;2.

Rudnick, D. L., 2016: Ocean research enabled by underwater gliders. *Annu. Rev. Mar. Sci.*, **8**, 519–541, doi:10.1146/annurev-marine-122414-033913.

Shay, L. K., and R. L. Elsberry, 1987: Near-inertial ocean current response to Hurricane Frederic. *J. Phys. Oceanogr.*, **17**, 1249–1269, doi:10.1175/1520-0485(1987)017<1249:NIOCRT>2.0.CO;2.

——, G. J. Goni, and P. G. Black, 2000: Effects of a warm oceanic feature on Hurricane Opal. *Mon. Wea. Rev.*, **128**, 1366–1383, doi:10.1175/1520-0493(2000)128<1366:EOAWOF>2.0.CO;2.

Shulman, I., and Coauthors, 2009: Impact of glider data assimilation on the Monterey Bay model. *Deep-Sea Res. II*, **56**, 188–198, doi:10.1016/j.dsr2.2008.08.003.

Soloviev, A. V., R. Lukas, M. A. Donelan, B. K. Haus, and I. Ginis, 2014: The air–sea interface and surface stress under tropical cyclones. *Sci. Rep.*, **4**, 5306, doi:10.1038/srep05306.

Tallapragada, V., and Coauthors, 2015: Hurricane Weather Research and Forecasting (HWRF) model: 2015 scientific documentation. Developmental Testbed Center, 113 pp. [Available online at http://www.dtcenter.org/HurrWRF/users/docs/scientific_documents/HWRF_v3.7a_SD.pdf.]

Wang, C., and S.-K. Lee, 2007: Atlantic warm pool, Caribbean low-level jet, and their potential impact on Atlantic hurricanes. *Geophys. Res. Lett.*, **34**, L02703, doi:10.1029/2006GL028579.

Wang, X., G. Han, Y. Qi, and W. Li, 2011: Impact of barrier layer on typhoon-induced sea surface cooling. *Dyn. Atmos. Oceans*, **52**, 367–385, doi:10.1016/j.dynatmoce.2011.05.002.

Wang, Y., and C.-C. Wu, 2004: Current understanding of tropical cyclone structure and intensity changes—A review. *Meteor. Atmos. Phys.*, **87**, 257–278, doi:10.1007/s00703-003-0055-6.

Yablonsky, R. M., and I. Ginis, 2009: Limitation of one-dimensional ocean models for coupled hurricane–ocean model forecasts. *Mon. Wea. Rev.*, **137**, 4410–4419, doi:10.1175/2009MWR2863.1.

Yaremchuk, M., D. Nechaev, and C. Pan, 2011: A hybrid background error covariance model for assimilating glider data into a coastal ocean model. *Mon. Wea. Rev.*, **139**, 1879–1890, doi:10.1175/2011MWR3510.1.

Zhang, W. G., J. L. Wilkin, and H. G. Arango, 2010: Towards an integrated observation and modeling system in the New York Bight using variational methods. Part I: 4DVAR data assimilation. *Ocean Modell.*, **35**, 119–133, doi:10.1016/j.ocemod.2010.08.003.